Appl Phys B (2010) 99: 409–414
DOI 10.1007/s00340-010-3963-4

Applied Physics B
Lasers and Optics

Femtosecond diode laser MOPA system at 920 nm based on asymmetric colliding pulse mode-locking

T. Ulm · A. Klehr · G. Erbert · F. Harth · J.A. L'huillier

Received: 26 November 2009 / Revised version: 17 February 2010 / Published online: 16 March 2010

Abstract We report on the generation of 267 fs long pulses with a peak power of 661 W emitted by an InGaAs diode laser master-oscillator power-amplifier (MOPA) system with an external grating compressor. The oscillator emits strongly chirped picosecond pulses with several nanometer of bandwidth, which can be amplified without significant phase modulation and are compressed to femtosecond pulses after leaving the amplifier. We used a diode laser module for asymmetric colliding pulse mode-locking and optimized the collision point and the relative intensity of the counter-propagation pulses.

1 Introduction

A new generation of small and energy-saving femtosecond lasers could open up new fields of applications for ultrafast lasers, for example imaging in biosciences [1] or medical applications [2]. For more than two decades—see [3] for a review—femtosecond lasers based on electrically pumped diode lasers have been investigated. The main drawback of the existing short pulse diode lasers is their—compared to ultrafast solid-state lasers [4, 5]—limited peak power.

In spite of large progresses have been achieved in the field of cw diode lasers, the generation and amplification of mode-locked pulses still remains a complicated task, because short carrier lifetimes and self-phase modulation effects decreases the performance of diode lasers in mode-locked operation [6, 7]. Usually chirped pulse amplification (CPA) is used in order to increase the output power and to prevent unwanted non-linear effects in amplifiers [8, 9]. Unfortunately stretcher set-ups between oscillator and amplifier inhibit an integration of semiconductor components on a single chip. In order to achieve further reduction in complexity and production costs of short pulse diode lasers, we developed a MOPA system with a master oscillator generating pulses with a strong frequency chirp [10]. As the pulse width is several picoseconds long, no additional stretcher is required before amplification. The large spectral bandwidth of several nanometers is sufficient for the generation of femtosecond pulses by an external grating compressor.

In literature the generation of sub-ps pulses with diode lasers using colliding pulse mode-locking (CPML) has been reported since 1991 [11]. In contrast to these previous investigations on the field of CPML, we now demonstrate the benefit of CPML for the formation of strongly chirped ps pulses and the tailoring of the chirp for a following amplification and compression. This new approach is described in detail in Sect. 4. In this paper we report on the generation of femtosecond pulses with a asymmetric colliding pulse mode-locked diode laser system combined with an external compressor. We investigated the influence of several operational parameters with the aim to optimize the chirp of the oscillator pulses with respect to the following amplification and compression stages. For the first time (to our knowledge) we investigated the influence of two parameters that turned out to be significant for the generation of a strong and nearly linear chirp: First, the collision point of the circulating pulses relative to the absorber position. We used single stripe lasers with asymmetric sectioning for these experiments. Second,

T. Ulm (✉) · F. Harth · J.A. L'huillier
Photonik-Zentrum Kaiserslautern e.V., Kohlenhofstr. 10,
67663 Kaiserslautern, Germany
e-mail: thorsten.ulm@pzkl.de

A. Klehr · G. Erbert
Ferdinand-Braun-Institut für Höchstfrequenztechnik,
Gustav-Kirchhoff-Str. 4, 12489 Berlin, Germany

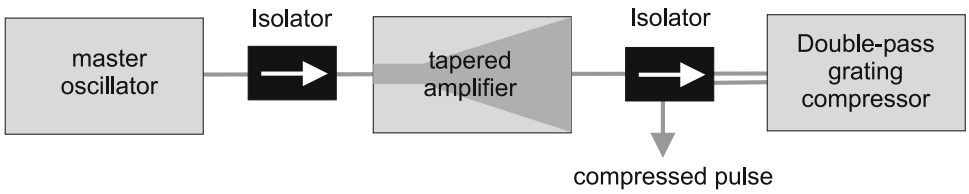

Fig. 1 Sketch of the experimental setup consisting of master oscillator, tapered amplifier and pulse compressor

we optimized the influence of the relative intensities of the colliding pulses.

2 Experimental setup

Figure 1 shows a sketch of the experimental setup, consisting of an oscillator in a linear cavity, a tapered amplifier and a double-pass grating compressor [12]. The key component of the master oscillator is a 920 nm two-section ridge-waveguide-laser (RW-laser) with one gain and one absorber section (see Fig. 2). The layer structure was grown using metalorganic vapor-phase epitaxy (MOVPE) and soldered epi-side up on a C-mount. The active region consists of an InGaAs double quantum well (QW) embedded in GaAsP spacer layers. The p- and n-doped 1800 nm thick $Al_{0.45}Ga_{0.55}As$ wave-guide layers are sandwiched between 450 nm $Al_{0.70}Ga_{0.30}As$ cladding layers.

On the top of the structure is a highly doped p-GaAs contact layer. The electrical contact of the waveguide is divided into a 1220 µm long gain section and a 80 µm long absorber section at the end of the wave-guide. Chemical composition and epitaxial structure of both sections are identical. A reverse voltage bias applied to the absorber section controls the absorption and saturation characteristics [13, 14].

Due to the super large optical cavity (SLOC) structure of the 3600 nm thick waveguide layers, the vertical far field angle is reduced to 20° (FWHM). The lasers have a ridge waveguide for the lateral mode confinement with an effective index step of $\Delta n_{\text{eff}} = 5 \times 10^{-3}$. The width of the ridge is 3 µm. The front and back facets of the laser used in this experiments are anti-reflection coated with a residual reflectivity of $R \leq 5 \times 10^{-4}$.

Two collimation lenses of 4.5 mm focal length are placed at both ends of the waveguides. The coupling efficiency was estimated to 40%. The external cavity is formed by two flat mirrors with reflectivity R_g next to the gain section and R_a next to the absorber section. The external cavity increases the pulse repetition time and allows the absorption to recover completely before the next pulse arrives. This prevents an unstable or chaotic behavior as observed by Yousefi et al. [15]. An optical isolator was inserted to prevent reflections from the amplifier input facet to reach the oscillator. Continuously emitting MOPA systems had been operated successfully without an optical isolator using a graded index lens between oscillator and amplifier [16]. However, pulsed systems might require a more critical alignment to achieve an undisturbed mode-locking.)

For amplification a tapered amplifier was used. The laser structure for the tapered amplifier is formed by an InGaAs single quantum well embedded in GaAsP spacer layers and 800 nm thick AlGaAs n- and p-waveguide layers. The tapered amplifier consists of a 700 µm long index-guided straight section and a 2000 µm gain-guided tapered section. The index guiding is achieved by a ridge waveguide formed by reactive ion etching and depositing of an insulator on the etched surface. The ridge width is 3 µm. The metallization on the p-side contact was formed by evaporating a Ti-Pt-Au multilayer and by electro-plating a thick Au layer. After thinning and n-metallization the wafer was cleaved to a total length of $L = 2750$ µm. The devices used in the experiments have a total taper angle of $\varphi = 6°$. The front and rear facets were anti-reflection coated ($R \leq 5 \times 10^{-4}$). The devices were mounted epi-side down on CuW submounts using AuSn. This subassembly was soldered on C-mounts using PbSn. The n-side was contacted by wire bonding.

To compensate for the astigmatism caused by the different diffraction angles along the slow (horizontal) and fast axis (vertical) a combination of a 4.5 mm collimator lens and a cylindrical lens of 80 mm focal length is used.

After leaving the amplifier the pulses enter the grating compressor. We used gratings with 1800 grooves per mm blazed for a wavelength of 1000 nm manufactured by *Spectrogon*. The gratings are optimized to be used in Littrow configuration. The diffraction efficiency is 94% and optimized for the first order. The compressor contains a non-magnifying telescope assembled of two 200 mm plan-convex lenses mounted on a translation stage together with two folding mirrors. Depending on the position of this stage the group-delay dispersion (GDD) of the compressor has a positive or negative sign. Therefore the sign and amount of the linear chirp can be obtained from the compressor geometry. An end mirror sends the pulse backwards through the compressor on the same path is has moved forwards to eliminate the spatial chirp introduced by the gratings.

A second optical isolator protects the tapered amplifier from back reflections and is used to separate the counter-propagating compressed pulses from the amplified pulses. The output beam is guided to the beam diagnostics afterwards.

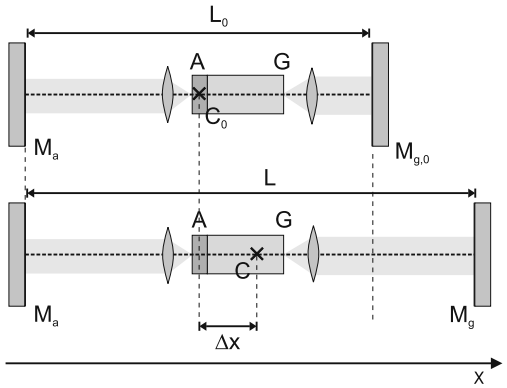

Fig. 2 The pulse collision point can be shifted by moving one of the mirrors of the external resonator. For the definition of labels see text

3 Collision point measurement

Depending on the location of pulse collision the strong saturation of gain or absorption has different impact on the pulse shaping within the master oscillator. Usually the sections in CPML diode lasers are aligned that way, that the pulses collide within the absorber [17]. This situation is depicted in the upper part of Fig. 2, where the absorber section is placed at the cavity center. Since the absorber length (80 µm) is much smaller than the pulse length (≈500 µm) the absorber length can be neglected and its position is denoted by A. The collision occurs in the center (C) of the optical path L between the mirrors M_a and M_g.

If the pulses collide inside the absorber section the rapid generation of new charge carriers leads to a decrease of the refractive index. If the collision occurs inside the gain section, the depletion of the inversion results in an increasing refractive index. Neither amplitude nor phase changes arise from a pulse collision in air, i.e. outside the wave-guide. The dynamics of the refractive index changes is closely connected to the frequency chirp of the pulse [18]. Therefore we expect a significant influence of the collision point on the chirp of the pulse. Instead of moving the diode laser module, we shifted the external resonator mirrors to move the collision point inside the wave-guide. As the absolute value of the repetition rate is not critical in our experiments the cavity length does not have to be constant. Therefore we shifted the collision point by moving mirror M_g and kept M_a fixed.

Before we can start optimizing the collision point, we need to have a suitable method to determine its position. Because the diode laser is kept in a housing for dust protection, we cannot measure the distance between cavity center and absorber section directly. Further, as the pulse is only 0.5 mm long within the wave-guide we require a method with sub-mm accuracy. As a reference point for this measurement we use the absorber position. For a proper colliding pulse mode-locking the collision point (C) has to be at—or at least close to—the absorber section (A) (see Fig. 2).

The upper part of Fig. 2 shows a cavity configuration with the absorber section located at the collision point C_0. Since C_0 is the center point of the optical path length L_0 between the mirrors, the relation

$$\overline{M_a A} = \frac{1}{2} L_0 \tag{1}$$

holds. If the right mirror is moved outwards (as depicted in the lower part of Fig. 2), the collision point C shifts to the right to a distance of Δx from the absorber. The absorber is now bleached twice: one time by the clockwise and one time by the counter-clockwise propagation pulse. If the temporal separation of both pulses is longer than the recovery time (≈10 ps), this causes a formation of satellite pulses that can be clearly observed in the autocorrelation trace. The delay Δt of satellite and main pulse is given by

$$2n\Delta x = c\Delta t, \tag{2}$$

with n denoting the refractive index of the waveguide ($n \approx 3.6$). The center point of the cavity with length L is now located at C and therefore the relation

$$\overline{M_a A} + n\Delta x = \frac{1}{2} L \tag{3}$$

holds. Solving this relation for Δx we achieve together with (1)

$$\Delta x = \frac{1}{2n}(L - L_0) = \frac{c}{2n}\left(\frac{1}{\nu_{\mathrm{rep}}} - \frac{1}{\nu_{\mathrm{rep},0}}\right). \tag{4}$$

$\nu_{\mathrm{rep}} = c/L$ denotes the pulse repetition frequency. Note that, since two pulses propagate inside the cavity, the pulse repetition frequency is twice the fundamental repetition frequency of the cavity. Together with (2) we obtain from (4) the equation

$$\Delta t = T - T_0. \tag{5}$$

When the cavity is shortened by moving M_g inwards, the collision point moves out of the wave-guide and the pulses collide in air. For this case we although achieve (4), if we set $n = 1$. Δx becomes negative, if the pulses collide outside the wave-guide.

With (4) the separation Δx of collision point and absorber section can be calculated from the repetition frequency ν_{rep}, if $\nu_{\mathrm{rep},0}$ is known and as long as we keep the mirror M_a fixed. For the repetition rate $\nu_{\mathrm{rep},0}$ the pulses meet at the absorber section and Δx becomes zero. If Δx is larger that the pulse length, its value can be determined directly form the autocorrelation trace by measuring the delay Δt of main and satellite pulse and using (2). $\nu_{\mathrm{rep},0}$ can therefore be obtained from Fig. 3, which shows the satellite pulse delay Δt for different repetition times T. At a repetition rate

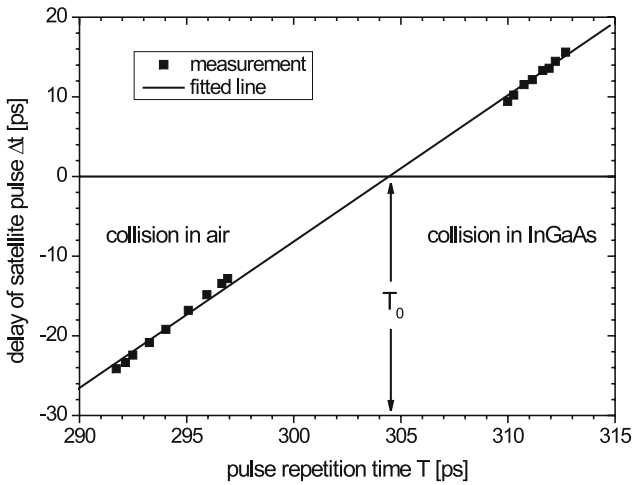

Fig. 3 Delay Δt between satellite pulse and main pulse for different positions of the cavity mirror next to the gain section. The shift of this mirror causes a shift of the collision point and changes the cavity round-trip time T

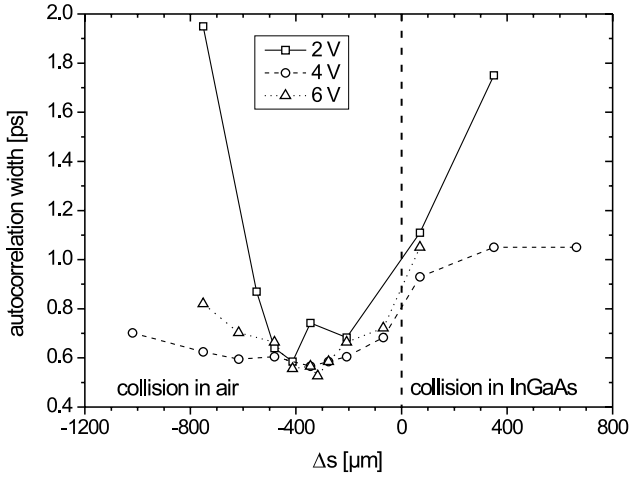

Fig. 4 FWHM of the autocorrelation function of the compressed pulse for different optical path lengths Δs between collision point and absorber

of $\nu_{\mathrm{rep},0} = 3.285$ GHz the pulses collide exactly within the absorber section.

Figure 3 shows the linear dependency of Δt and T. The inclination of the line is not equal to one, as predicted by (5), but has a value of 1.8. In our opinion this is caused by the fact that the absorber remains transparent up to 10 ps after a pulse has passed. Therefore a larger delay of the main and the satellite pulse occur. Further, a pulse pair with larger delay experiences more gain, because the larger delay allows more gain to be build up after the passage of the first pulse.

4 Collision point optimization

With a method for calculating the collision point in reference to the absorber location, we started optimizing Δx by shifting the output coupling mirror M_g. To treat the collision in air and in InGaAs equally, we introduce the optical path length

$$\Delta s = n\Delta x = \frac{c}{2}\left(\frac{1}{\nu_{\mathrm{rep}}} - \frac{1}{\nu_{\mathrm{rep},0}}\right) \tag{6}$$

derived from (4). The mirror reflections are $R_g = 30\%$ and $R_a = 99.3\%$. To obtain stable mode-locking we apply a DC reverse bias voltage in the range of 2–6 V to the absorber section. The injection current to the gain section is 100 mA. The current applied to the tapered amplifier is 4 A and the amplifier is operated at gain saturation. The repetition rate changes from 3.16 to 3.42 GHz depending on the position of mirror M_g. For each value of Δx the pulse compressor is optimized to the shortest pulse duration after compression. The 2 V curve (see Fig. 4) shows an irregular shape with two minima. There is no much difference between the minimal pulse duration achieved with 4 V and 6 V. We choose a reverse voltage of 4 V for further experiments, to limit the current load of the absorber section.

Figure 4 clearly shows that the optimized collision point is located in air, approximately 400 μm away from the absorber at the end of the wave-guide. As discussed before gain and absorption saturation cause different phase changes. If the collision point is located near the absorber but inside the gain section, both gain and absorption saturation influences the temporal phase of the pulse. This leads to a rather complicated, non-quadratic spectral phase that cannot be compensated by the grating compressor. If the pulses collide in air near the absorber, the absorber gives the pulse a strong up-chirp. The power density in the gain section is much smaller than in the first case and the phase changes are mainly influenced by the absorber section. This leads to a nearly quadratic spectral phase and a nearly linear chirp.

In the next step we optimized the reflectivity of the cavity mirrors R_g and R_a in order to further decrease the duration of the compressed pulse. From various combinations of R_g and R_a the values $R_g = R_a = 40\%$ yield the shortest pulses after compression. The pulse characteristics for the optimized cavity are presented and discussed in the following section.

5 Pulse compression results

Figures 5(a), 5(b) and 5(d) show the autocorrelation functions (ACF), the optical spectra and the RF spectra of the shortest pulse achieved in our experiments using CPML. The oscillator gain current was 120 mA, the reverse absorber voltage was 4 V. The oscillator emits a pulse train with a repetition rate of 3.326 GHz and an average output power

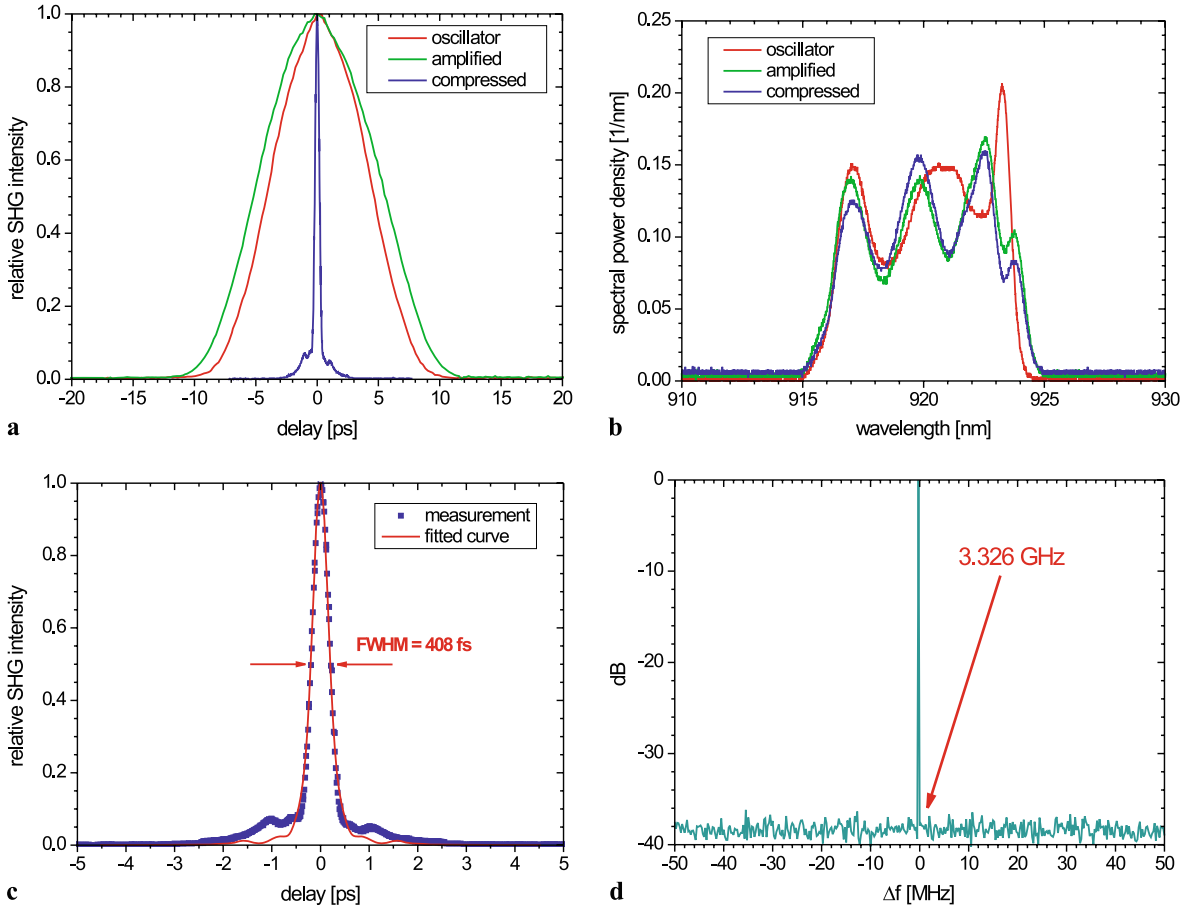

Fig. 5 (**a**) Autocorrelation functions and (**b**) spectra of the pulses measured behind the oscillator, tapered amplifier and grating compressor. (**c**) Measured and fitted autocorrelation function of the compressed pulse. (**d**) Rf spectrum of the pulse train after pulse compression. For further details see text

of 20 mW. Assuming a Gaussian shaped pulse a pulse duration of 6.2 ps can be obtained from the FWHM of the ACF. The calculated peak power and pulse energy is 0.9 W and 6 pJ. The counter-propagating pulses collide in air, 563 µm behind the absorber section. The pulses are 1.8 mm long in air and the collision point is close enough to the absorber to assure a pulse overlap within the absorber. This leads to a stable colliding pulse mode-locking.

The tapered amplifier increases the average power to 1.45 W. The pulse is slightly elongated to 7.6 ps, but the ACF is still of Gaussian shape. The peak power reaches 54 W and the pulse energy rises to 436 pJ. Due to diffraction losses at the compressor gratings and transmission losses inside the optical isolator the average power after compression is 708 mW.

As can be seen form Fig. 5(c) the ACF of the compressed pulse is not equal neither to a Gaussian nor a sech^2 shape. In order to retrieve the true pulse duration from the ACF an estimation of the pulse shape is made using the spectrum $S(\omega)$ of the compressed pulse. Note that the measured spectrum $S(\omega)$ represents the spectral intensity, not the electrical field. In the first step of the calculation, we assume a constant spectral phase and calculate the shortest possible pulse that can be formed from the spectrum $S(\omega)$ via the Fourier transformation. This bandwidth-limited pulse $I_S(t)$ would be 148 fs long.

As the second step the intensity autocorrelation $A_S(\tau)$ is calculated from $I_S(t)$ for a set of delay times τ. The FWHM of $A_S(\tau)$ is 223 fs. The relation of pulse duration and autocorrelation width is 0.6604, which is close to the value for sech^2 pulses (0.6482). The measured ACF of the compressed pulse is broader due to high order spectral phase terms.

In the third step the maximum of both, the measured and the calculated ACF, is normalized to a value of one. The calculated ACF $A_S(\tau)$ is fitted to the measured ACF $A_M(\tau)$ by stretching it along the delay (τ) axis. The fitted ACF is in good agreement with the measured ACF near the center of the pulse. From the FWHM of the fitted ACF (408 fs) a pulse duration of 267 fs can be obtained. The pulse duration is 1.8 times above the Fourier limit (148 fs). This is a good result if we consider that a grating compressors compensates

only for the group-delay dispersion, but not for higher order dispersion terms [19].

The measured ACF indicates a small satellite pulse at a delay of approximately 1 ps. This delay agrees well with the spectral maxima with a separation of 2.74 nm, that can be seen in the spectra of the amplified and compressed pulse. This means that the satellite pulse is created in the MOPA system and is not an artefact of pulse compression. Therefore the pulse forming process in the MOPA system requires further and more detailed investigations using phase-sensitive measurements (e.g. SHG-FROG [19]) in the future.

From the compressor geometry we obtained a positive GDD for the pulses generated by the MOPA system. Therefore the compression could also be achieved simply by a pair of diffraction gratings, which allows a compact compressor set-up.

The peak power after compression is dependent of the pulse shape, which is described by the pulse shape factor F^*. From $I_S(t)$ we obtained a value of $F^* = 0.8296$. This shows the similarity of the compressed pulse to a sech^2-pulse ($F^* = 0.8814$) predicted by the theory of passive mode-locking [20]. Assuming that the bandwidth-limited pulse $I_S(t)$ has the same shape as the real pulse we calculated a peak power of 661 W for the compressed pulse. After pulse compression a pulse energy of 213 pJ was achieved.

In Fig. 5(d) the RF spectrum of the compressed pulse train is shown. Since there is neither broadening of the RF signal nor side bands, we conclude that the amplitude modulation is less than 36 dB and the timing jitter is less than 1 MHz.

6 Conclusion

We have demonstrated a diode laser MOPA system for a wavelength of 920 nm combined with an external grating compressor. The oscillator was optimized for the generation of strongly chirped picosecond pulses with a sufficiently large spectral bandwidth to generate femtosecond pulses with an external pulse compressor. Since no stretcher is required before the tapered amplifier this system is suitable for a integration of oscillator and amplifier on a single semiconductor chip. For pulse generation colliding pulse mode-locking in a diode laser module with asymmetric sectioning was used. We investigated the influence of the collision point and the cavity losses on the pulse shaping in order to achieve a nearly linear chirp and short pulses after compression. The optimum collision point is located in air, $\approx$400 µm away from the absorber. For cavity mirror reflections of $R_g = R_a = 40\%$ we obtained the shortest pulses of 267 fs duration, an average power of 708 mW, a peak power of 661 W and a pulse energy of 213 pJ at a repetition rate of 3.3 GHz.

Acknowledgements The authors would like to thank Richard Wallenstein for his continuous support and many helpful discussions. This work was funded by the German "Federal Ministry of Education and Research" (project number: 13 N 8568).

References

1. W.R. Zipfel, R.M. Williams, W.W. Webb, Nat. Biotechnol. **21**, 1369 (2003)
2. A. Vogel, J. Noack, G. Hüttman, G. Paltauf, Appl. Phys. B **81**, 1015 (2005)
3. K.A. Williams, M.G. Thompson, I.H. White, New J. Phys. **6**, 179 (2004)
4. E. Sorokin, I.T. Sorokina, E. Wintner, Appl. Phys. B **72**, 3 (2001)
5. C.T.A. Brown, M.A. Cataluna, A.A. Lagatsky, E.U. Rafailov, M.B. Agate, C.G. Leburn, W. Sibbett, New J. Phys. **6**, 175 (2004)
6. A. Dienes, L.W. Carr, J. Appl. Phys. **69**, 1766 (1991)
7. D.J. Derickson, R.J. Helkey, A. Mar, J.R. Karin, J.G. Wasserbauer, J.E. Bowers, IEEE J. Quantum Electron. **28**, 2186 (1992)
8. P.J. Delfyett, A. Dienes, J.P. Heritage, M.Y. Hong, Y.H. Chang, Appl. Phys. B **58**, 183 (1994)
9. K. Kim, S. Lee, P.J. Delfyett, Opt. Express **13**, 4600 (2005)
10. T. Ulm, F. Harth, H. Fuchs, J.A. L'huillier, R. Wallenstein, Appl. Phys. B **92**, 481 (2008)
11. Y.K. Chen, M.C. Wu, T. Tanbun-Ek, R.A. Logan, M.A. Chin, Appl. Phys. Lett. **58**, 1253 (1991)
12. O.E. Martinez, IEEE J. Quantum Electron. **23**, 59 (1987)
13. A.M. Fox, D.A.B. Miller, G. Livescu, J.E. Cunningham, W.Y. Jan, IEEE J. Quantum Electron. **27**, 2281 (1991)
14. D.A.B. Miller, D.S. Chemla, T.C. Dames, A.C. Gossard, W. Wiegmann, T.H. Wood, C.A. Burrus, Phys. Rev. B **32**, 1043 (1985)
15. M. Yousefi, Y. Barbarin, S. Beri, E.A.J.M. Bente, M.K. Smit, R. Nötzel, D. Lenstra, Phys. Rev. Lett. **98**, 044101 (2007)
16. S. Schwertfeger, A. Klehr, G. Erbert, G. Tränkle, IEEE Photonics Technol. Lett. **16**, 1268 (2004)
17. M.C. Wu, Y.K. Chen, T. Tanbun-Ek, R.A. Logan, M.A. Chin, G. Raybon, Appl. Phys. Lett. **57**, 759 (1990)
18. R.S. Grant, W. Sibbett, Appl. Phys. Lett. **58**, 1119 (1991)
19. J.-C. Diels, W. Rudolph, *Ultrashort Laser Pulse Phenomena*, 2nd edn. (Academic Press/Elsevier, San Diego/Amsterdam, 2006)
20. H.A. Haus, IEEE J. Quantum Electron. **6**, 1173 (2000)